

# Photocuring and Photolithography of Proton-Conducting Polymers Bearing Weak and Strong Acids

Jennifer Schmeisser and Steven Holdcroft\*

Department of Chemistry, Simon Fraser University, Burnaby, British Columbia, V5A 1S6, Canada

Jianfei Yu, Tran Ngo, and Ged McLean

Angstrom Power Inc., 980 W. First Street, No. 106, North Vancouver,  
British Columbia, V7P 3N4, Canada

Received June 8, 2004. Revised Manuscript Received November 1, 2004

A series of novel conformable proton-conducting thin films has been prepared from photocurable liquid polyelectrolytes. Films prepared in such a fashion show promise for engineering unconventionally shaped proton-exchange membranes using photolithographic techniques. These films are semi-interpenetrating networks (semi-IPN) comprising a linear proton-conducting guest polymer, sulfonated poly[ether ether ketone] (S-PEEK), in the presence of a statistically cross-linked host polymer matrix comprising divinyl sulfone, vinylphosphonic acid, and acrylonitrile. Film properties ranging from brittle and fragile to robust and flexible have been obtained, depending on the ratio of host/guest composition used. The extent of dissociation of the weak acid component, vinylphosphonic acid, is strongly dependent on the S-PEEK content. Proton conductivity, water content, and  $\lambda$  values are dependent on the membrane composition and degree of cross-linking. Proton conductivities similar to those of pure S-PEEK,  $\sim 0.07$  S/cm, have been observed for a semi-IPN containing as little as 35 wt % S-PEEK.

## 1. Introduction

The proton-exchange membrane (PEM) is a key component of solid polymer electrolyte fuel cells. It acts as both a separator to prevent mixing of reactant gases, and as an electrolyte for transporting protons from anode to cathode.<sup>1–3</sup> Nafion is the most widely studied PEM because it exhibits high conductivity, good mechanical strength, and chemical stability, and is commercially available. Nonfluorinated and partially fluorinated hydrocarbon-based membranes are viewed as low-cost alternatives to Nafion.<sup>4,5</sup> Sulfonated poly(arylenes) such as sulfonated poly[ether ether ketone] (S-PEEK) are under intense investigation.<sup>6–8</sup> They are easily prepared with well-defined ion-exchange capacities (IECs), are generally soluble in organic solvents, possess good proton conductivity, thermal and chemical stability, and exhibit good performance in  $H_2$  and methanol/air fuel cells.<sup>9,10</sup>

Conventionally, Nafion and sulfonated polyarylenes are employed as pre-cast or pre-molded membranes and com-

pressed between two catalyzed electrodes under elevated temperature to form membrane–electrode assemblies (MEA) to achieve good interfacial adhesion. However, the requirement of using preformed membranes may restrict new fuel cell processing designs where high temperature and high pressure must be avoided. For instance, novel fuel cell design concepts might require the PEM to be conformable by injection molding, formed as microchannels and unique shapes, or strongly adhering to the catalyst layer without hot pressing. One conceptual route to enhance processability of PEMs is to prepare viscous liquids that can be cast, printed, or sprayed as films or as microstructured designs, and subsequently photocured, thermally cured, or cured by electron beam irradiation. Within this concept, a plausible demonstration is to dissolve a preformed proton-conducting polymer in a vinyl monomer/cross-linking agent, and to polymerize this composition to form a semi-IPN in which one polymer is cross-linked in the presence of a linear polymer (the proton-conducting polymer) as shown in Figure 1.<sup>11</sup> The difficulty, however, is finding suitable monomers capable of dissolving the ionic proton-conducting material.

In this work a series of semi-interpenetrating networks (semi-IPNs) of proton-conducting membranes are formed by photocuring of polymerizable liquids comprising linear S-PEEK, acrylonitrile (ACN), vinylphosphonic acid (VPA), divinyl sulfone (DVS), and dimethylacetamide (DMA) (Figure 2). S-PEEK was chosen as the proton-conductive medium because of its solubility in a variety of solvents and

\* To whom correspondence should be addressed. E-mail: holdcrof@sfu.ca.

- (1) Appleby, J.; Foulkes, R. L. *Fuel Cell Handbook*; Van Nostrand: New York, 1989.
- (2) Prater, K. J. *Power Sources* **1990**, 29, 239–250.
- (3) Srinivasan, S. J. *Electrochem. Soc.* **1989**, 136 (2), C41–C48.
- (4) Savadogo, O. J. *New Mater. Electrochem. Syst.* **1998**, 1 (1), 47–66.
- (5) Rikukawa, M.; Sanui, K. *Prog. Polym. Sci.* **2000**, 25, 1463–1502.
- (6) Wang, F.; Hickner, M.; Ji, Q.; Harrison, W.; Mecham, J.; Zawodzinski, T. A.; McGrath, J. E. *Macromol. Symp.* **2001**, 175, 387–396.
- (7) Wang, F.; Hickner, M.; Kim, Y. S.; Zawodzinski, T. A.; McGrath, J. E. *J. Membr. Sci.* **2002**, 197, 231.
- (8) Hasiotis, C.; Li, Q. F.; Deimede, V.; Kallitsis, J. K.; Kontoyannis, C. G.; Bierrum, N. J. *J. Electrochem. Soc.* **2001**, 148 (5), A513–A519.
- (9) Zaidi, S. M. J.; Mikhailenko, S. D.; Robertson, G. P.; Guiver, M. D.; Kaliaguine, S. *J. Membr. Sci.* **2000**, 173, 17–34.
- (10) Inzelt, G.; Pineri, M.; Schultze, J. W.; Vorotyntsev, M. A. *Electrochim. Acta* **2000**, 45, 2403–2421.

- (11) Klempner, D.; Berkowski, L. Interpenetrating Polymer Networks. In *Encyclopedia of Polymer Science and Engineering*; Wiley-Interscience: New York, 1987; pp 279–341.

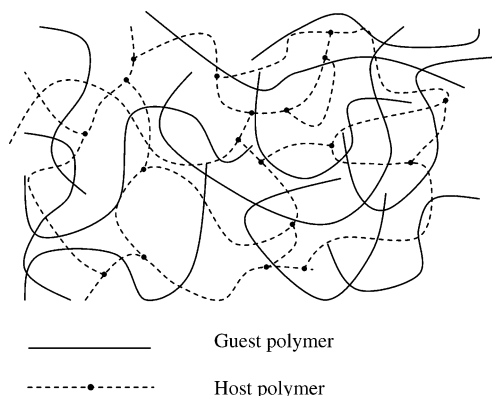


Figure 1. Schematic of semi-IPN.

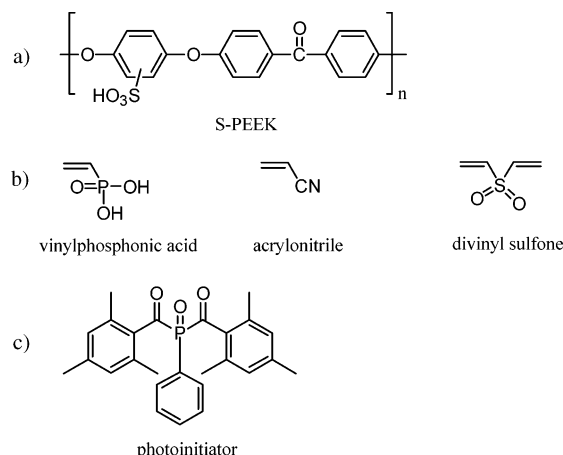


Figure 2. Chemical structures of (a) S-PEEK, (b) host monomers, and (c) photoinitiator.

because its IEC can be controlled by adjusting reaction parameters.<sup>9</sup> These particular monomers were chosen primarily because of their ability to solvate S-PEEK and because of their functionality: ACN provides flexibility and reduces brittleness of photocured films; VPA has been shown to enhance proton conductivity when polymerized into PEMs;<sup>12</sup> DVS for its cross-linking ability; and DMA reduces the viscosity of the liquid solution. Thus, a cross-linked matrix comprising VPA, DVS, and ACN is considered the host polymer, and S-PEEK is the guest. The effect of the composition of the photocurable liquid on IEC, proton conductivity, water content, lambda values, thermal decomposition,  $T_g$ , and optical clarity of the resultant films are presented.

## 2. Experimental Section

**2.1 Materials.** PEEK, poly[ether ether ketone], (Vitrex  $M_n \approx 110\,000$  g/mol), concentrated sulfuric acid (Anachemia), vinylphosphonic acid (Aldrich), and dimethylacetamide (Aldrich) were used as received. Divinyl sulfone (DVS) and acrylonitrile (ACN) were obtained from Aldrich and distilled prior to use. The photoinitiator, bis(2,4,6-trimethylbenzoyl)-phenylphosphine oxide (IRGACURE 819), was provided courtesy of Ciba Specialty Chemicals Canada Inc. and used as received.

**2.2 Preparation of S-PEEK Homopolymer.** A series of S-PEEK polymers was prepared by dissolving 18 g of PEEK in

Table 1. Compositions of Liquid Polyelectrolytes (wt %)

sample	S-PEEK	VPA	DVS	AN	PI	DMA
Varying S-PEEK Content						
S1	0	19	44	19	3	16
S2	4	17	43	17	3	15
S3	8	17	41	17	3	15
S4	17	15	37	15	3	13
S5	31	13	31	13	2	11
Varying DVS Content						
S6	26	9	18	33	2	12
S7	26	9	25	25	2	12
S8	26	9	32	18	2	12
S9	26	9	41	9	3	12

300 mL of concentrated sulfuric acid overnight at room temperature followed by reaction at 50–55 °C for 6.5 h.<sup>13</sup> Films of 70–150- $\mu\text{m}$  thickness were prepared by dissolving S-PEEK (~25 wt %) in DMSO and casting onto a glass plate. Cast membranes were dried at 90 °C overnight and subsequently washed in deionized water to remove residual solvent.

The degree of sulfonation (DS) of S-PEEK was determined by <sup>1</sup>H NMR spectroscopy of 3 wt % S-PEEK/DMSO-*d*<sub>6</sub> solutions,<sup>13</sup> and found to be 74%.

**2.3 Preparation of Photocurable Polyelectrolytes.** Photocurable polyelectrolytes were prepared according to the compositions shown in Table 1. To a 20-mL vial the appropriate amounts of liquid monomer (VPA, DVS, ACN), solvent (DMA), and photoinitiator (PI) were added. All samples were sealed and kept in the dark at room temperature for 12 h to ensure dissolution of the initiator. To another 20-mL vial an appropriate amount of S-PEEK was added and the corresponding solution of monomer/solvent/PI mixture was added. Complete dissolution of the S-PEEK in the monomer mixture took ~2 days at room temperature. The viscosity of the resulting clear yellow solutions varied from free flowing to honey-like syrup as the S-PEEK content increased.

**2.4 UV Photocured Electrolytes.** Thin films of each solution were spread with a casting knife onto glass slides fitted with Cu wire (150  $\mu\text{m}$ ) spacers. The wires were 75 mm long and separated by 23 mm. The liquids were cured by irradiation using an ELC-500 (Electro-Lite Corp., Danbury, CT) light-exposure chamber fitted with four 9-W visible lamps which generate broad spectrum visible light, 410–520 nm, centered at 450 nm. Films were situated inside the chamber at approximately 10 cm from the light source and cured for up to 4 h or until they were no longer tacky. Photocured films were stored in Milli-Q water. Cured film thicknesses ranged from 70 to 150  $\mu\text{m}$ , depending on the Cu wire thickness.

**2.5 Characterization.** Infrared spectroscopy was performed on a Bomen BM-Series FT-IR spectrometer. UV–visible absorption spectra were recorded on a Cary 3E spectrophotometer. Ion exchange capacities of photocured films were determined by direct titration of triplicate samples to the phenolphthalein endpoint. The titrated ion exchange capacities were then used to estimate  $\lambda$ , typically defined as  $[\text{H}_2\text{O}]/[\text{SO}_3^-]$ , but in this case defined as  $[\text{H}_2\text{O}]/[\text{acid site}]$  to reflect the presence of more than one distinct acid groups that can be associated with water in the membrane. Film thicknesses were measured using a micrometer ( $\pm 0.001$  mm, Mitutoyo) and sample diameters were measured using a caliper ( $\pm 0.1$  mm, Mitutoyo).

Thermal decomposition temperatures for the homopolymers and semi-IPNs were determined using thermogravimetric analysis (TGA) on a Shimadzu TGA-50 thermogravimetric analyzer. Samples of dry films of ~2–5 mg were placed in platinum pans and heated from 25 to 500 °C at a rate of 10 °C/min under ambient atmosphere.

(12) Florjanczyk, Z.; Wielgus-Barry, E.; Poltarzewski, Z. *Solid State Ionics* **2001**, *145*, 119–126.

(13) Huang, R. Y. M.; Shao, P.; Burns, C. M.; Feng, X. *J. Appl. Polym. Sci.* **2001**, *82*, 2651–2660.

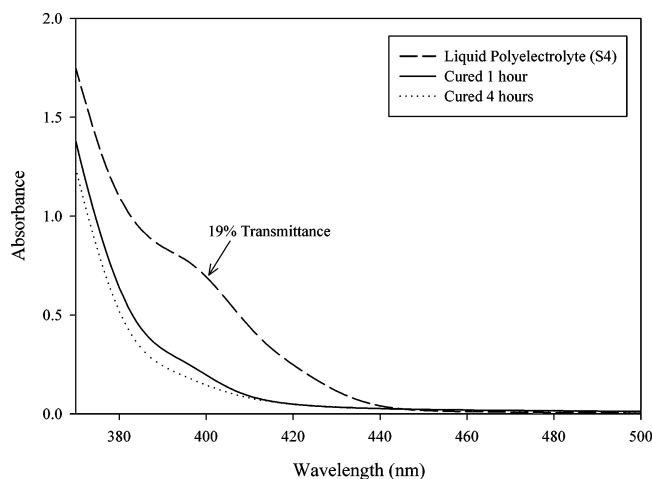


**Figure 3.** UV absorption spectra of Sample S4, 17 wt % S-PEEK, liquid, and photocured polyelectrolyte.

Differential scanning calorimetry (DSC) using a DSC Q10 (TA Instruments) was used to determine the glass transition,  $T_g$ , of the pure host/guest polymers and photocured semi-IPNs. The instrument was first calibrated against indium. Samples of dry films ( $\sim 2$ – $10$  mg) were placed in aluminum DSC pans and heated under a nitrogen atmosphere at a rate of  $10$   $^{\circ}\text{C}/\text{min}$  from  $20$  to  $150$   $^{\circ}\text{C}$  and held at  $150$   $^{\circ}\text{C}$  for  $10$  min to remove residual water. The samples were cooled from  $150$  to  $-100$   $^{\circ}\text{C}$  and melting thermograms were obtained at a constant heating rate of  $10$   $^{\circ}\text{C}/\text{min}$  from  $-100$  to  $250$   $^{\circ}\text{C}$ . The data were analyzed using Universal Analysis 2000, version 3.7A.

Proton conductivity was determined by a.c. impedance spectroscopy with a Hewlett-Packard 8753A network analyzer (Agilent Technologies) and analyzed with Z-view (Scribner Associates) using a technique previously described.<sup>14</sup> The average of three samples is reported.

**2.6 Fuel Cell Polarization Curves.** Commercial H-TEC (Luebeck, Germany) electrodes were used to evaluate the UV-cured semi-IPN membranes and a sample of Nafion 117 for comparison. The as-received electrodes were used to prepare membrane-electrode assemblies (MEA) simply by clamping the electrolyte of interest between two  $16\text{-cm}^2$  electrodes. The MEA was positioned into an H-TEC single cell fixture and installed into an in-house fuel cell (FC) test station. The cell was operated at room temperature and fed with unhumidified  $\text{H}_2$  at the anode at a flow rate of  $50$  mL/minute and unhumidified air at the cathode at a flow rate of  $100$  mL/minute.

### 3. Results and Discussion

**3.1 Spectroscopic Analyses.** The UV–Vis absorption spectrum of the photocurable solution extends from the UV to  $450$  nm as illustrated in Figure 3 for a thin liquid film ( $70$   $\mu\text{m}$ ) containing  $17$  wt % S-PEEK (Sample S4). A broad absorption peak can be seen, as a shoulder between  $385$  and  $415$  nm, due to the absorption of the photoinitiator. The transmittance at  $\lambda_{\text{max}}$  of the initiator ( $400$  nm) is  $19\%$  and hence may be irradiated uniformly throughout the thickness of the liquid film. The incident light source, while having maximum power at  $450$  nm, emits a broad spectrum of light between  $410$  and  $520$  nm, sufficient to photodegrade the

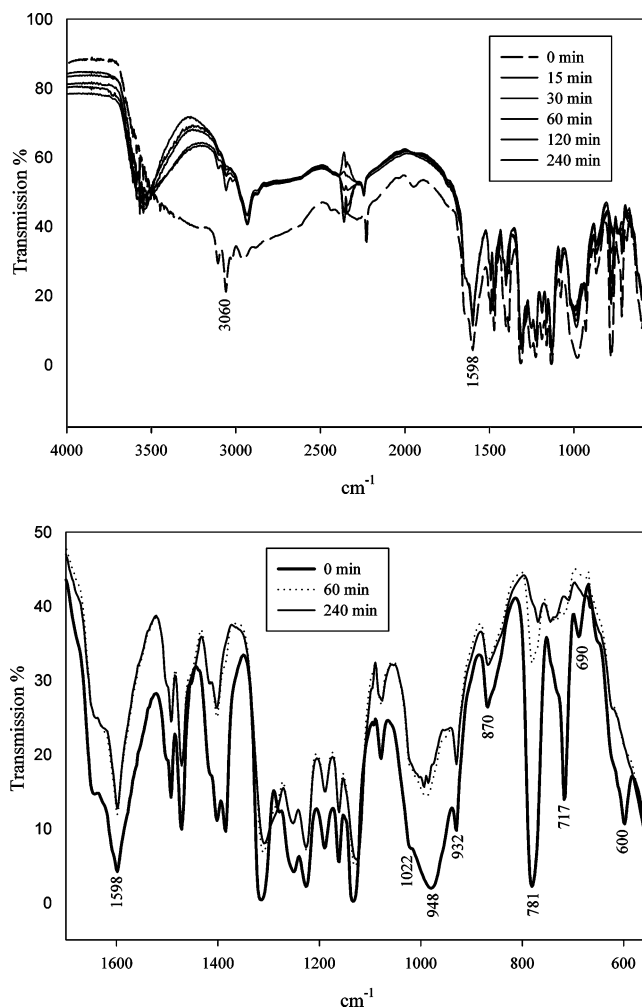


**Figure 4.** IR spectrum of Sample S4, 17 wt % S-PEEK: (a) composite, and (b) fingerprint region.

initiator. Also shown in Figure 3 is the evolution of the UV–Vis absorption spectrum as a function of photocure time. The loss of the  $385$ – $415$  nm shoulder corresponds to photolysis of the photoinitiator.

The resulting photocured polyelectrolytes are assumed to be semi-IPNs with S-PEEK playing the role of the linear guest polymer residing in a cross-linked random copolymer of VPA, ACN, and DVS host. To confirm that the polymerization proceeds as expected, changes in the FTIR spectrum of the photocurable solutions were monitored in situ. A small amount of the sample,  $<1$  mg, was sandwiched between two  $6\text{-mm}$  NaCl plates (Aldrich) and the IR spectrum was recorded between  $4000$  and  $550$   $\text{cm}^{-1}$  at  $16$  scans resolution. FTIR spectra were obtained periodically after  $0$ ,  $15$ ,  $30$ ,  $60$ ,  $120$ , and  $240$  min. curing time. Figure 4a shows the evolution of the FTIR spectra for the  $17$  wt % S-PEEK (Sample S4). A more detailed picture of the fingerprint region is included in Figure 4b showing only  $0$ ,  $60$ , and  $240$  min. curing times for clarity. IR spectra of S-PEEK and pure unreacted monomers were obtained and used as reference in assigning the peaks for the polymerizable mixture.

The number of components, and similarity between the functional groups, in the polymeric solution renders the IR spectrum complex, and hence accurate identification of each peak is difficult. Rather, groups of peaks, in characteristic

(14) Beattie, P. D.; Orfino, F. P.; Basura, V. I.; Zychowska, K.; Ding, J.; Chuy-Sam, C.; Schmeisser, J. M.; Holdcroft, S. *J. Electroanal. Chem.* **2001**, *503*, 45–56.

**Table 2. Effect of Curing Time on Proton Conductivity of Sample S4, 17 wt % S-PEEK, Photocured Semi-IPN**

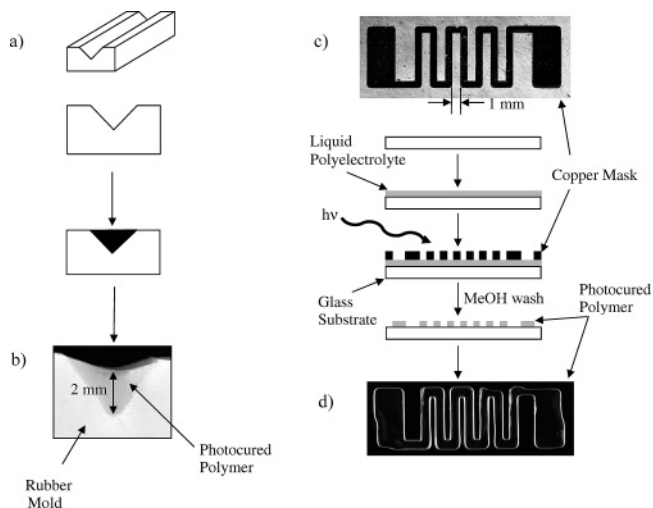
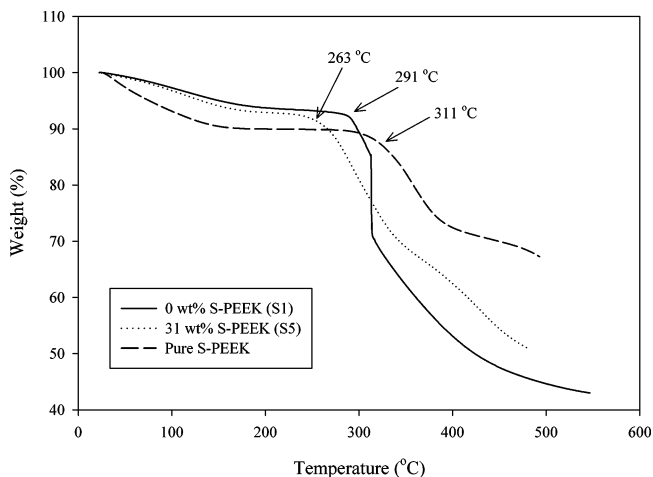
UV cure time (min)	conductivity (S/cm)
15	0.033
60	0.041
90	0.043
120	0.049
180	0.050
240	0.050

frequency ranges, corresponding to specific functional groups were monitored with curing time. The broad peak centered at  $3060\text{ cm}^{-1}$ , attributed to the hydrogen bonding between the phosphonic acid groups and present in the FTIR spectrum of pure VPA, diminishes rapidly. This is considered due to a decrease in hydrogen bonding as VPA is incorporated into the cross-linked structure. Although the characteristic vinyl ( $\text{C}=\text{C}$ ) stretch expected at  $\sim 1610\text{ cm}^{-1}$  is masked by the large broad peak at  $1598\text{ cm}^{-1}$ , due to S-PEEK, there is a decrease in peak size attributed to the consumption of the vinyl groups. Further evidence of vinyl group consumption comes from the decrease in all peaks between  $1000$  and  $550\text{ cm}^{-1}$ , characteristic of the out-of-plane bending modes ( $-\text{CH}=\text{CH}_2$ ) for all monosubstituted monomers. This evidence indicates that the monomers are consumed and that cross-linking has taken place.

**3.2 Effect of Curing Time on Conductivity.** To determine the minimum photocuring time required for curing, a series of 17 wt % samples (Sample S4) were prepared and cured for 15, 60, 90, 120, 180, and 240 min. Each sample was immediately submersed in water after the allotted cure time to stop the photocuring reaction. Three samples representing each curing time were cut and their proton conductivity at room temperature was measured. As can be seen in Table 2 there is only minimal improvement in conductivity (0.03 to 0.05 S/cm) when the cure time is increased from 15 min to 1.5 h. Curing for longer than 1.5 h has neither a positive or negative effect on proton conductivity.

**3.3 Conformability.** Thin films of each composition listed in Table 1 were readily photocured into solid materials by irradiation with 450 nm light. To illustrate that the polyelectrolyte solutions can be photocured into unique shapes a sample was cured in a V-shaped mold, see Figure 5a, which was constructed from soft rubber. The liquid was poured into the mold, the excess overflow was removed with a casting knife, and the polyelectrolyte was cured in the UV chamber at 450 nm for 1 h. A photograph of the cross section of the cured electrolyte in the mold is shown in Figure 5b. Although the electrolyte fills the gap entirely there is noticeable shrinkage upon curing as can be seen by the concavity on top of the sample. Little change in shape and/or concavity is observed after soaking the sample in water for several days.

To illustrate that the polyelectrolyte can be spatially cured a sample was spread ( $\sim 70\text{-}\mu\text{m}$  thickness) onto a glass slide, which had been rendered opaque by spray painting black on one side, and the copper mask, shown in Figure 5c, placed overtop. The slide was then cured for 15 min and the uncured monomers were washed away with methanol. The resulting imaged film is shown in Figure 5d.

**Figure 5.** (a) Schematic of the rubber mold, (b) photograph of cross section of cured electrolyte in the mold, (c) copper mask, and (d) photolithographically cured film.**Figure 6.** TGA of Samples S1, S5, and pure S-PEEK (0, 31, and 100 wt % S-PEEK, respectively).

**3.4 Thermal Analyses.** Thermogravimetric analysis was used to determine the decomposition temperatures for pure S-PEEK and the photocured films. Figure 6 shows thermograms for 0, 31, and 100 wt % S-PEEK samples (S1, S5, and S-PEEK, respectively). All films show an  $\sim 10$  wt % decrease between 50 and  $200\text{ }^{\circ}\text{C}$  due to loss of residual water. Desulfonation commences at  $311\text{ }^{\circ}\text{C}$  for pure S-PEEK which is consistent with literature values for S-PEEK of similar IEC.<sup>9</sup> Decomposition of the pure host polymer and the 31 wt % S-PEEK semi-IPN begins at 291 and  $263\text{ }^{\circ}\text{C}$ , respectively. The combination of host and guest causes the semi-IPN to decompose at lower temperatures than each of the separate components. This has also been observed in composite materials where an interaction exists between functional groups on the component polymers.<sup>15</sup> For instance, it is speculated that a pseudo-hydrogen bond between the C-H groups on PVDF (polyvinylidene fluoride) and the C=O groups on PVP (poly(vinylpyrrolidone)) catalyzes the thermal decomposition of PVDF/PVP composites leading to a decrease in observed decomposition temperature. A similar



**Table 3. Thermal Properties of Samples S1, S5, and Pure S-PEEK (0, 31, and 100 wt % S-PEEK, Respectively)**

sample	S-PEEK content (wt %)	$T_d$ (°C)	$T_g$ (°C)
S1	0	291	
S5	31	263	195
S-PEEK	100	311	198

argument can be made here in regards to the decreased thermal stability observed for the semi-IPN materials, i.e., degradation is facilitated by pseudo-hydrogen bonding between the carbonyl group on S-PEEK and the P—O—H group present on VPA.

DSC measurements were used to determine glass transition temperatures for the 0, 31, and 100 wt % S-PEEK samples, listed in Table 3. S-PEEK exhibits a clear  $T_g$  at 198 °C consistent with the literature.<sup>9</sup> For the 31 wt % S-PEEK semi-IPN there appears to be a very subtle  $T_g$  at about 195 °C. For the 0 wt % S-PEEK, pure host polymer, no clear  $T_g$  can be seen. Two possible explanations exist: (1) either the  $T_g$  is broad and the DSC method is not sensitive enough to detect it, or (2) the  $T_g$  is located above the decomposition temperature,  $T_d$ . More detailed thermal characterization of this polymer is currently underway.

**3.5 Ion Exchange Capacity.** In an electrolyte that contains only strong acid groups that fully dissociate in water, such as  $-\text{SO}_3\text{H}$  ( $\text{p}K_a \approx -0.6$ ), the theoretical IEC,  $\text{IEC}^{\text{theo}}$ , may be calculated simply from knowing the proportion of sulfonic acid sites within the polymer. This value, termed degree of sulfonation (DS), is defined in eq 1 and can be determined by integrating the  $^1\text{H}$  NMR spectrum. The DS of S-PEEK used in this study is 74%, and the ion exchange capacity,  $\text{IEC}^{\text{theo}}$  ([mmol  $\text{SO}_3\text{H}$  units]/[g dry polymer]), determined using eq 2<sup>13</sup> was calculated to be 2.04 mmol/g.

$$\text{DS} = \frac{(\text{molar no. of the PEEK}-\text{SO}_3\text{H unit})}{(\text{molar no. of the PEEK}-\text{SO}_3\text{H unit}) + (\text{molar number of the PEEK unit})} \quad (1)$$

$$\text{IEC}^{\text{theo}} = \frac{1000\text{DS}}{288 + 102\text{DS}} \quad (2)$$

The  $\text{IEC}^{\text{theo}}$  and the IEC determined by titration,  $\text{IEC}^{\text{exp}}$ , usually agree very well, when all the protons are accessible to titration. This is the case for S-PEEK, for which  $\text{IEC}^{\text{exp}}$  was found to be 2.14 mmol/g compared to an  $\text{IEC}^{\text{theo}}$  of 2.04 mmol/g, as listed in Table 4.

In principle, in blends of S-PEEK,  $\text{IEC}^{\text{theo}}$  can be determined from the S-PEEK mass fraction in the blend. However, in the present case a weak diprotic acid, vinylphosphonic acid ( $\text{p}K_{a1} \approx 1.70$ ,  $\text{p}K_{a2} \approx 7.10$ ),<sup>16</sup> is introduced as a second proton source. According to acid–base equilibria theory the fraction of weak acid that dissociates to release charge-carrying protons is dependent on the acid concentration. In the presence of the strong sulfonic acid of S-PEEK, a large fraction of the weak acid is calculated to be undissociated—although still titratable. Thus, since titration registers all protons, dissociated and undissociated, this

method overestimates the number of protons available for conductivity.

A more appropriate estimation of the free protonic carrier concentration in these films is the *effective* IEC ( $\text{IEC}^{\text{eff}}$ ), i.e., mmol of dissociated  $\text{H}^+$  in water swollen films per gram of dry polymer. To calculate these values the assumption is made that sulfonic acid of S-PEEK is fully dissociated. Thus, the proton concentration due to the dissociation of S-PEEK can be estimated according to eq 3

$$[\text{H}^+] = \frac{W_d \cdot W\%_{\text{S-PEEK}} \cdot \text{IEC}_{\text{S-PEEK}}^{\text{exp}}}{V_w \cdot 1000} \quad (3)$$

where  $W_d$  is the sample dry weight (mg),  $W\%_{\text{S-PEEK}}$  is the weight percent S-PEEK in the sample,  $\text{IEC}_{\text{S-PEEK}}^{\text{exp}}$  is the ion exchange capacity of S-PEEK (mmol/g) determined by titration, and  $V_w$  is the wet sample volume ( $\text{cm}^3$ ).  $[\text{H}^+]$  for the 0 wt % S-PEEK was determined using the autodissociation of water at neutral pH. The corresponding fraction of undissociated VPA and dissociated VPA, due to both the first and second dissociation, are approximated using eqs 4, 5, and 6.

$$\text{Degree of undissociated VPA: } \alpha_{\text{H}_2(\text{VPA})} = \frac{[\text{H}^+]^2}{[\text{H}^+]^2 + [\text{H}^+] \cdot K_{a1} + K_{a1} \cdot K_{a2}} \quad (4)$$

$$\text{Degree of first dissociation: } \alpha_{\text{H}(\text{VPA})^-} = \frac{K_{a1} \cdot [\text{H}^+]}{[\text{H}^+]^2 + [\text{H}^+] \cdot K_{a1} + K_{a1} \cdot K_{a2}} \quad (5)$$

$$\text{Degree of second dissociation: } \alpha_{(\text{VPA})^{2-}} = \frac{K_{a1} \cdot K_{a2}}{[\text{H}^+]^2 + [\text{H}^+] \cdot K_{a1} + K_{a1} \cdot K_{a2}} \quad (6)$$

Except for films which contain no S-PEEK (Sample S1),  $\alpha_{(\text{VPA})^{2-}}$  was calculated to be negligible ( $<10^{-7}$ ).  $\text{IEC}^{\text{eff}}$  values for cured polyelectrolyte films were calculated according to eq 9 using the contributions from S-PEEK and VPA, calculated using eq 7 and 8, respectively, and are included in Table 2. For comparison,  $\text{IEC}^{\text{exp}}$  values determined by titration, are also included.

$$\text{IEC}_{\text{S-PEEK}}^{\text{eff}} = (W\%_{\text{S-PEEK}} \cdot \text{IEC}_{\text{S-PEEK}}^{\text{exp}}) \quad (7)$$

$$\text{IEC}_{\text{VPA}}^{\text{eff}} = \alpha_{\text{H}(\text{VPA})^-} \left( \frac{W\%_{\text{VPA}}}{MW_{\text{VPA}} \cdot 1000} \right) \quad (8)$$

$$\text{IEC}^{\text{eff}} = (\text{IEC}_{\text{VPA}}^{\text{eff}} + \text{IEC}_{\text{S-PEEK}}^{\text{eff}}) \quad (9)$$

where  $W\%_{\text{VPA}}$  is the weight percent of VPA, and  $MW_{\text{VPA}}$  is the molecular weight of VPA (mol/g).

$\text{IEC}^{\text{eff}}$  values are observed to be much lower than the corresponding values obtained by titration, confirming that titration is an inappropriate technique for evaluating systems incorporating weak acids.

(16) *Dictionary of Organic Compounds*, 5th ed.; Chapman and Hall: New York, 1982.

Table 4. Effect of S-PEEK Content on Properties of Photocured Film, Samples S1–S5

sample	S-PEEK (wt %)	VPA (wt %)	(IEC <sup>eff</sup> <sub>S-PEEK</sub> ) <sup>a</sup> (mmol/g)	( $\alpha_{H(VPA)-}$ ) <sup>b</sup>	(IEC <sup>eff</sup> <sub>VPA</sub> ) <sup>c</sup> (mmol/g)	(IEC <sup>eff</sup> <sub>total</sub> ) <sup>d</sup> (mmol/g)	(IEC <sup>exp</sup> ) <sup>e</sup> (mmol/g)	water content (wt %)	$\lambda$ ([H <sub>2</sub> O]/[acid site])	[H <sup>+</sup> ] <sup>f</sup> M	$\sigma$ <sup>g</sup> (S/cm)
S1	0	19		0.56	0.98	0.98	1.14	54	37		0.015
S2	4	17	0.09	0.34	0.54	0.63	1.94	46	34	0.30	0.015
S3	8	17	0.17	0.19	0.28	0.45	1.98	44	29	0.23	0.023
S4	17	15	0.34	0.13	0.18	0.52	2.31	66	35	0.21	0.040
S5	31	13	0.61	0.06	0.08	0.69	2.12	58	37	0.36	0.070
S-PEEK	100	0	2.04 <sup>h</sup>			2.14	2.14	36	15	1.52	0.066

<sup>a</sup> Contribution of S-PEEK to IEC<sup>eff</sup> calculated using eq 7. <sup>b</sup> Using eq 5. <sup>c</sup> Contribution of VPA to IEC<sup>eff</sup>, calculated using eq 8. <sup>d</sup> IEC<sup>eff</sup>, calculated using eq 9. <sup>e</sup> Determined by titration. <sup>f</sup> Based on free proton concentration calculated using eq 10. <sup>g</sup> “Wet” films measured at 25 °C. <sup>h</sup> IEC<sup>theo</sup>, calculated using eq 2.

Once IEC<sup>eff</sup> is calculated, the total proton concentration, [H<sup>+</sup>]<sub>Total</sub>, taking into account all dissociated protons can be calculated using eq 10

$$[H^+]_{\text{Total}} = \frac{(IEC^{\text{eff}} \cdot W_d / V_w)}{1000} \quad (10)$$

where  $W_d$  and  $V_w$  are the dry weight (mg) and the wet volume (cm<sup>3</sup>) of the sample, respectively.

**3.6 Effect of S-PEEK Content on Photocured Composition Membranes.** Samples S1–S5 were prepared to determine the effect of varying the S-PEEK content in the films while maintaining a constant ratio between the host polymer components. The upper limit for S-PEEK content is 31 wt % S-PEEK, which is the limit of S-PEEK solubility in the mixture of monomers.

The mechanical properties of the films vary greatly across the series and depend on both the S-PEEK content and hydration level of the semi-IPN. When wet, films with low S-PEEK content are very brittle and break easily, whereas high S-PEEK content films are much more flexible and robust. When dry, membranes containing a high content of S-PEEK are slightly more flexible than those containing low content, although generally all dry membranes crack easily.

IEC, proton conductivity, and water content data are shown in Table 4. For purposes of comparison, values of IEC<sup>eff</sup>,  $\lambda$ , and [H<sup>+</sup>] are listed in Table 4. The experimental value of [H<sup>+</sup>] for S1 could not be calculated because it was too brittle and its volume could not be measured.

As the S-PEEK content is increased (from 0 to 17 wt %) IEC<sup>eff</sup> drops. Upon a further increase (from 17 to 31 wt %) IEC<sup>eff</sup> increases. This trend is explained by considering the separate contributions of S-PEEK and VPA. The contribution to IEC<sup>eff</sup> from S-PEEK, calculated based on the degree of sulfonation and S-PEEK content in the semi-IPN, increases linearly from 0.00 to 0.61 mmol/g with S-PEEK content (see Figure 7); whereas the contribution to IEC<sup>eff</sup> from VPA decreases nonlinearly from 0.98 to 0.08 mmol/g over the same S-PEEK content increase. Because these two opposing trends do not occur at the same rate there is a nonlinear relationship between total IEC<sup>eff</sup> and S-PEEK content.

In addition to there being no clear relationship between IEC<sup>exp</sup> and IEC<sup>theo</sup>, Figure 8 shows that there is no clear relationship between S-PEEK content and water content (nor  $\lambda$ ). The only thing to note is that the water contents and  $\lambda$  values are much higher for the semi-IPN materials (44–58 wt % H<sub>2</sub>O,  $\lambda$  = 29–37) than for the pure S-PEEK materials

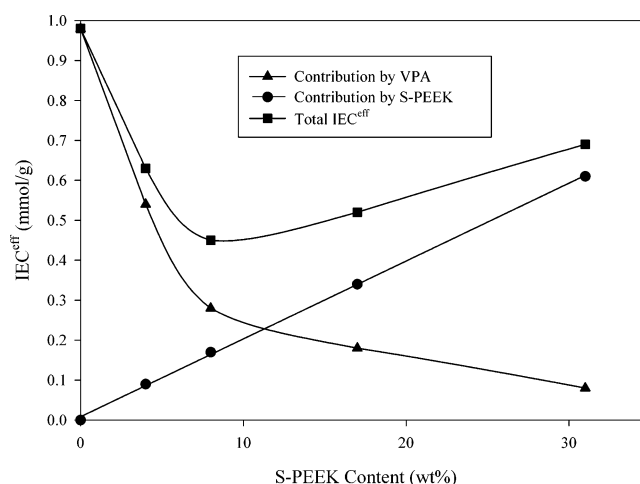


Figure 7. Contribution of S-PEEK and VPA to IEC<sup>eff</sup> as a function of S-PEEK content, Samples S1–S5.

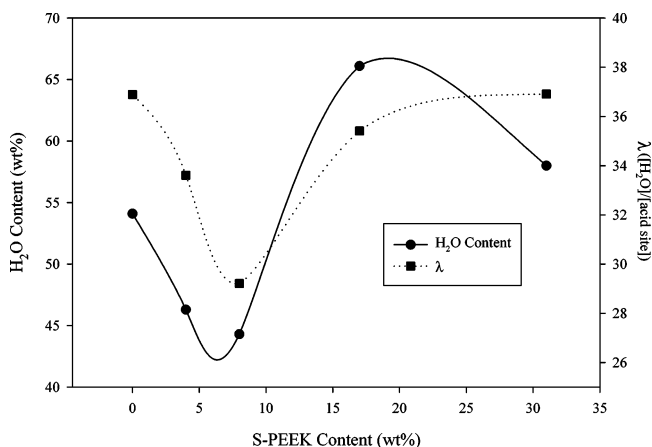


Figure 8. Effect of S-PEEK content on H<sub>2</sub>O content and  $\lambda$ , Samples S1–S5.

(36.2 wt % H<sub>2</sub>O,  $\lambda$  = 15) due to their having a larger percentage of hydrophilic groups compared to pure S-PEEK.

Even without S-PEEK present the host polymer exhibits a measurable conductivity (0.015 S/cm) because of the presence of the secondary proton source, VPA. A minimum of at least 8 wt % S-PEEK is required for any further increase in conductivity as shown in Figure 9. Above 8 wt %, conductivity increases linearly with S-PEEK content up to a value of 0.07 S/cm for the 31 wt % S-PEEK semi-IPN.

An interesting observation is that the proton conductivity of the 31 wt % S-PEEK semi-IPN is identical to the conductivity of the S-PEEK homopolymer, 0.07 S/cm, particularly since the [H<sup>+</sup>] within the samples is quite different, 0.36 M vs 1.52 M. Since the contribution of VPA

Table 5. Effect of Cross Linking/DVS Content on Photocured Semi-IPN Films

	DVS <sup>a</sup> content (wt %)	(IEC <sup>eff</sup> <sub>S-PEEK</sub> ) <sup>b</sup> (mmol/g)	( $\alpha_{\text{H(VPA)}}^-$ ) <sup>c</sup>	(IEC <sup>eff</sup> <sub>VPA</sub> ) <sup>d</sup> (mmol/g)	(IEC <sup>eff</sup> <sub>total</sub> ) <sup>e</sup> (mmol/g)	(IEC <sup>exp</sup> ) <sup>f</sup> (mmol/g)	water content (wt %)	$\lambda$ ([H <sub>2</sub> O]/ [acid site])	[H <sup>+</sup> ] <sup>g</sup> M	$\sigma^h$ (S/cm)
S6	18	0.52	0.08	0.07	0.59	2.18	55	31	0.93	0.056
S7	25	0.52	0.07	0.06	0.58	1.99	49	27	1.00	0.048
S8	32	0.52	0.07	0.06	0.58	1.80	45	25	0.94	0.035
S9	41	0.52	0.06	0.05	0.56	1.47	35	20	0.94	0.025

<sup>a</sup> For full composition see Table 1. <sup>b</sup> Contribution of S-PEEK to IEC<sup>eff</sup> calculated using eq 7. <sup>c</sup> Using eq 5. <sup>d</sup> Contribution of VPA to IEC<sup>eff</sup>, calculated using eq 8. <sup>e</sup> IEC<sup>eff</sup>, calculated using eq 9. <sup>f</sup> Determined by titration. <sup>g</sup> Based on free proton concentration calculated using eq 10. <sup>h</sup> "Wet" films measured at 25 °C.

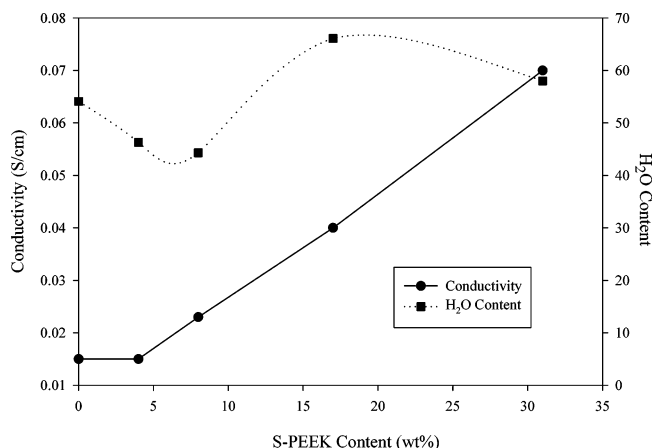


Figure 9. Effect of S-PEEK content on proton conductivity and H<sub>2</sub>O content, Samples S1–S5.

to the free proton concentration is calculated to be negligible for this particular semi-IPN, this observation is believed a direct result of the higher  $\lambda$  value (37) and water content (58 wt %) in the semi-IPN film compared to the pure S-PEEK (36.2 wt % H<sub>2</sub>O,  $\lambda$  = 15).

**3.7 Effect of Cross-Linker (DVS) on Photocured Semi-IPN Membranes.** Semi-IPN films S6–S9, containing varying amounts of divinyl sulfone, were prepared to determine the effect of the cross-linker content on the physical properties of the semi-IPN films. To maintain a similar ion content throughout the series, the acrylonitrile content was decreased proportionally as the DVS content was increased. This provided a series of films possessing an S-PEEK content of 26 wt % and VPA content of 9 wt %. Results of IEC, proton conductivity, and water content measurements are shown in Table 5. For purposes of comparison, IEC<sup>eff</sup>,  $\lambda$ , and [H<sup>+</sup>] have been calculated and are included in Table 5.

The mechanical properties of the photocured semi-IPNs are similar across the series for both wet and dry membranes. All membranes are fairly robust when hydrated but brittle when dry.

Since the ion content is the same across the series, the contribution to IEC<sup>eff</sup> from S-PEEK and VPA, and hence overall IEC<sup>eff</sup> total, is approximately the same for all semi-IPN membranes. Given this, it might be expected that IEC<sup>exp</sup>, measured by titration, should be constant. However, as the DVS content is increased from 18 to 41 wt %, IEC<sup>exp</sup> decreases from 2.18 to 1.47 mmol/g. The water content also decreases from 54.9 to 34.8 wt % as a result of increasing the DVS content, Figure 10. This decreased water content is perceived due to a more cross-linked compact structure, which has less room to incorporate additional water molecules, and may render a fraction of the acidic sites

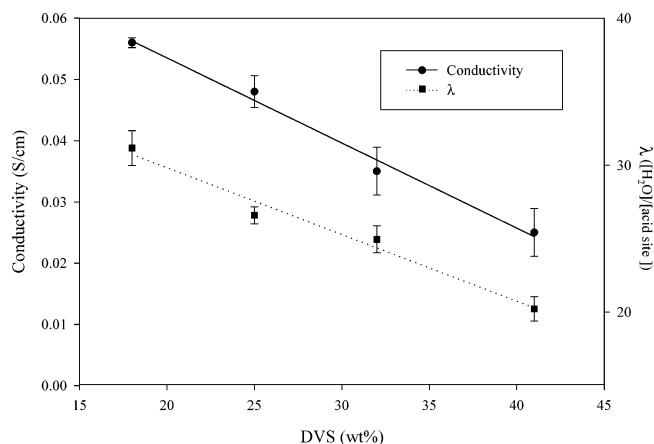


Figure 10. Effect of DVS content on proton conductivity and  $\lambda$ , Samples S6–S9.

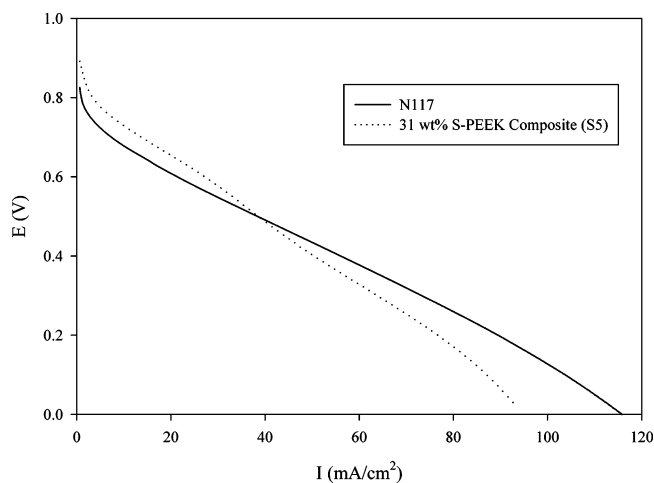


Figure 11. Fuel cell polarization curves for Nafion 117 and Sample S5 (31 wt % S-PEEK).

inaccessible to titration. As a direct result of this more compact structure, the semi-IPN conductivity decreases from 0.06 to 0.03 S/cm as DVS content increases, Figure 10.

**3.7 Fuel Cell Evaluation.** Preliminary fuel cell studies were performed to evaluate the semi-IPN membranes as possible electrolytes for use in room-temperature fuel cells. The cold contact formation of MEAs and unhumidified gas flow operating conditions were chosen to mimic fuel cell conditions of the intended application. Polarization data, Figure 11, were recorded once the cell had reached an open circuit voltage (OCV) of at least 0.75 V. When compared with N117, the S-PEEK semi-IPN (S5) shows higher performance in the kinetic region (>0.7 V), which may be explained by (i) a higher OCV, and (ii) a higher solubility of O<sub>2</sub> at the interface. Further studies are necessary to accurately interpret this result.

Lower current density of the S-PEEK semi-IPN at low cell potential is usually due to a decrease in the mass transport of O<sub>2</sub> in cathode and/or an increase in Ohmic resistance arising from membrane dehydration at the anode.

This fuel cell data shows that the cured semi-IPNs are reasonable candidates for further study, but much more work is required to optimize conditions to obtain good performance.

### 3. Conclusions

A series of novel photocurable liquid conformable polymer electrolytes have been prepared. The liquid polyelectrolytes are transformed into solid semi-IPN films by spreading the liquid onto a glass substrate and UV-curing.

Physicochemical properties of the films have been studied to understand the role of composition on proton conductivity. Conductivities similar to that of pure S-PEEK and Nafion 117, 0.07 S/cm,<sup>14</sup> have been achieved for a cured semi-IPN that contains as little as 31 wt % S-PEEK and 10 wt % VPA monomers.

Mechanical properties of these materials are directly related to the composition of the host polymer and the weight percent S-PEEK ionomer present. In general, materials containing low amounts of S-PEEK tend to be brittle and difficult to work with, whereas materials with high quantities of S-PEEK are more flexible and robust.

Properties such as water content,  $\lambda$ , [H<sup>+</sup>], and IEC are not linearly related to S-PEEK content, however conductivity is improved as S-PEEK content is increased. The degree of cross-linking, as controlled by the DVS content, has a significant impact on water content,  $\lambda$ , and conductivity.

Preliminary fuel cell studies show promise for photocured PEM use in room-temperature fuel cells. Further studies including MEA optimization for H<sub>2</sub>/air fuel cells are currently underway.

**Acknowledgment.** We are grateful to NSERC and Angstrom Power Inc. for financial support. We also thank Dr. Brad Easton and Dr. Titichai Navessin for useful discussions.

CM049083Z